UNIVERSITY OF TARTU

Faculty of Science and Technology

Institute of Technology

Silvar Muru

METHODS AND IMPLEMENTATION OF CONTAMINATION CONTROL ON MILREM ROBOTICS UGV SENSORS

Master's thesis (30 ECTS)

Robotics and Computer Engineering

Supervisor:

MSc Hendrik Ehrpais

Tartu 2021

Abstract

Methods and implementation of contamination control on Milrem Robotics UGV sensors

In this thesis two modules with different cleaning systems were designed. These modules contain the sensors and navigation lights used by the Milrem Robotics THeMIS UGV. The goal of the modules is to protect the sensors from external contamination and have the ability to clean the field-of-view of the camera in order to increase the image quality used by the onboard computer in autonomous mode. The modules also contain a set of sensors which are able to detect rain and mud on the outer surface. These sensors are used to initiate the cleaning system. A suitable method analysing the images before and after the cleaning was proposed. Lastly the method was put to use determining the best cleaning system designed. With these modules the UGV is able to get sensor data with better quality.

CERCS: T111 Imaging, image processing; T125 Automation, robotics, control engineering; T330 Military science and technology
Keywords: robotics, UGV, sensor contamination, camera analysis, blur

Milrem Robotics'i mehitamata maismaasõiduki sensorite puhastuse metoodikad ja rakendus

Magistritöö raames töötati välja kaks puhastussüsteemiga varustatud moodulit. Need moodulid sisaldavad Milrem Robotics'i THeMIS mehitamata maismaasõidukil kasutatavaid andureid ja navigatsiooni valgusteid. Moodulite eesmärk on kaitsta andureid välise saastumiste eest ja võimaldadab pardakaamera vaatevälja puhastamist, suurendamaks autonoomses režiimis kasutatavate piltide kvaliteeti. Lisaks sisaldavad moodulid ka andurite komplekti, mis on võimelised tuvastama välispinnale langenud vihma ja muda. Neid andureid kasutatakse puhastussüsteemi automaatseks käivitamiseks. Lisaks pakuti välja sobilik metoodika, millega analüüsida piltide hägususe astet. Lõpuks kasutati antud metoodikat, selgitamaks välja parim kavandatud puhastussüsteem. Loodud moodulite abil on sõidukil võimalik saada ümbritsevast keskkonnast parema kvaliteediga informatsiooni.

CERCS: T111 Pilditehnika; T125 Automatiseerimine, robootika, juhtimistehnika; T330 Sõjandus ja militaartehnoloogia
Võtmesõnad: robootika, mehitamata maismaasõiduk, saastunud sensor, kaamera analüüs, hägusus

Contents

Abstract **2**

List of Figures **5**

List of Tables **7**

Aberrations **8**

1 Introduction **9**

1.1 Milrem THeMIS UGV 10

1.2 Contamination control objectives 10

2 Proposed methods **12**

2.1 Contamination detection method 12

2.1.1 The rain detector 12

2.1.2 Solid particle detector 18

2.2 Cleaning efficiency method 19

2.2.1 Test setup requirements 20

2.2.2 Blur detection 22

3 Contamination control solutions **24**

3.1 Outer surface solutions 26

3.1.1 Wiper technology 28

3.1.2 Washing fluid system 29

3.1.3 Compressed air system 30

3.2 Inside surface systems 31

3.2.1 Glass heater 31

3.2.2 Moisture detection 33

4 Testing **34**

4.1 Detectors 35

4.1.1 Rain detector 36

4.1.2 Mud detector 37

4.2 Sensor analysis 38
4.2.1 Test setup 39
4.2.2 Software and test charts 39
4.2.3 Measurement results 40
4.3 Analysis and future work 42
Conclusion **44**
Acknowledgements **45**
Bibliography **46**
Appendices **50**
Appendix A - The rain detector module 50
Appendix B - The mud detector module 50
Non-exclusive licence **51**

List of Figures

2.1 Total internal reflection used in most car rain sensors [modified] 13

2.2 Rain detector module render 13

2.3 1 kHz pulse generator with IR LED (D1) 14

2.4 Transimpedance amplifier circuit 16

2.5 3D render of the custom-made sensor mainboard 18

2.6 Single photoresistor module 19

2.7 Solid particle detector assembly with four photoresistors 19

2.8 DUT, charts and lighting position 20

2.9 Render of the test setup 21

2.10 The Laplacian operator 23

3.1 Render of the front module 25

3.2 Render of the rear module 25

3.3 The front module enclosure components: main frame (1), shaft seal (2), shaft seal adapter (3), front window (4), CA3102E14S connector (5), back lid (6) 26

3.4 The front module enclosure components exploded view 27

3.5 Wiper module 28

3.6 Different wiper configurations [modified] 29

3.7 The washing fluid solution with water pump (1), water tank (2) and water nozzle (3) 30

3.8 Compressed air solutions with air pump (1) and air nozzle (2) 31

3.9 Heater module with heatwire [modified] 32

3.10 Heater module with camera mount - fan motor (1), heat element (2), temperature sensor (3), air funnel (4) and camera (5) 32

3.11 The DHT22 humidity sensor 33

4.1 Finished front modules 34

4.2 Finished rear module 35

4.3 Rain detector testing in a high light environment 36

4.4 Mud detector testing in a low light environment 37

4.5 Picture of the camera module 38

4.6 The test environment 39

4.7 Picture of the test chart before the test 40

4.8 Wiper against rain 41

4.9 Wiper against mud 41

4.10 Wiper and water sprinkler against mud 42

List of Tables

2.1 1 kHz pulse generator with IR LED components 15

2.2 Transimpedance amplifier components 17

3.1 Parameters of Polystyrene 28

Aberrations

3D	Three-dimensional
ADC	Analog-to-Digital Converter
COTS	Commercial off-the-shelf
DUT	Device under testing
FOV	Field-of-View
I_{FP}	Peak Forward Current
I_{FSM}	Forward Surge Current
IR	Infrared
LED	Light Emitting Diode
LiDAR	Light Distance and Range
LOS	Line of Sight
PCB	Printed Circuit Board
UGV	Unmanned Ground Vehicle
RGB	Red-Green-Blue
TIR	Total Internal Reflection
THeMIS	Tracked Hybrid Modular Infantry System

1 Introduction

Autonomous and unmanned ground vehicle (UGVs) platforms are the future to come [1, 2]. Even though most of the platforms are known to be mechanically robust enough to withstand most of the tasks given to the machine, there are still weak links in most of these systems [4, 5, 6]. One of those weak links is directly or relatively related to the sensors and autonomous capabilities [3, 5, 6].

The mechanical robustness is especially true for the Milrem Robotics UGVs which are designed to withstand the harshest environments where human presence is not suitable and in most cases can even be harmful [8]. The largest advantages of these types of platforms come when the machine is capable of making its own decisions and therefore has a launch-and-forget approach.

In order to achieve maximum safety and decision making the sensors must work in their optimal condition. This is especially valid for a UGV due to off-road conditions, where the existence of mud, dust and water puts the sensor's capabilities to the test. Therefore the requirements for these systems are much higher compared to systems that work in more controlled and predictable environments. Contaminated lenses, temperature fluctuations and undesirable levels of humidity are just some hazards which can affect the sensors' reliability and performance**.** Consequently this affects not being able to make a decision or even worse - making a wrong one. This can lead to serious damage to the machine or surrounding environment and even loss of the platform.

Human safety is one of the most critical topics in autonomous systems [9]. Unreliable decision making is currently a critical stepping stone for their wide implementation into environments with humans nearby [10, 14], even though robots and computers are often known to perform in many cases much more reliably, especially in monotone, boring and long-lasting tasks which can wear out an average human [11, 12]. Similarly to humans, in order to operate, robots also have to perceive its surroundings, which for a robot is done using cameras and LiDARs. With the help of artificial intelligence and computer vision algorithms the robot is sometimes able to detect and classify objects even better than humans [15, 16]**.**

When autonomous driving and sensor fusion and algorithms are more and more researched and getting better, solutions dealing with extrinsic hazards still need to be researched in

order to reduce the limitations of the environment the platforms are wished to perform. The purpose of this thesis is to conduct research which finds the suitable technical solutions to remove most common types of contaminations for off-road UGVs. Thus increasing the effectiveness of these algorithms with more sharp and realistic data to make better predictions.

1.1 Milrem THeMIS UGV

Milrem Robotics has been an Estonian manufacturer of UGVs in Tallinn and Tartu since 2013. Its main focus is to produce a state-of-the-art tracked hybrid powered unmanned platform whose modular design lets it be used with lots of different payloads. The company today is one of the world's leading manufacturers of its kind. The two main Milrem Robotics UGVs are called THeMIS for military applications and Multiscope for civil applications. [7]

THeMIS UGV with its modular design has remarkably versatile capabilities especially in off-road scenarios. With the help of other companies Milrem Robotics has developed 11 different fully functioning payloads with many coming in the future. The UGV can be used both in manual and in autonomous mode navigating in many different environments with upto 1.5 km LOS telelink. It is designed to withstand the roughest and most dangerous jobs and environments. Its autonomous mode is the key component reducing the human workload. It has six cameras and two LiDARs as sensors. [8] All of them are currently open to the elements and are constantly covered with mud and terrain that the tracks and the environment throw at them. Without sensors the machine is blind and needs to be controlled in line of sight by the operator.

Since 2018 the company and University of Tartu cooperated on a project called NUTIKAS. Its main focus is to develop new high-tech core autonomous capabilities in off-road scenarios [13]. One of the concerns is also sensor reliability to withstand the elements which this thesis helps to solve. Most of the development costs of this thesis were financed through this project.

1.2 Contamination control objectives

Reliable and accurate data from the cameras (and LiDARs) is used by the UGV to understand the surrounding environment to make predictions and motion planning in autonomous mode. The threat to the sensor's accuracy lies both in liquid and solid particles

which can contaminate the sensor's lens and create scattering, absence of information and worsen the overall image quality.

In autonomous mode the UGV currently has no system to determine if the information from the sensors is of good quality. Although the sensors locations and the likelihood of contamination is already minimized through the design of the machine, an extra layer of protection is needed to sustain its functions and mission regardless of the terrain and surroundings both in autonomous and manual mode. Without the autonomous mode the platform potential is limited by the operator's skills and view.

In manual mode the problem lies when the operator sees the contamination through the camera feed, but cannot remove it while driving teleoperationally. In addition to that the sensor module also consists of lights and indicators used in navigation and are placed out of the field-of-view (FOV) of the camera, making the operator not able to determine their cleanness through the video feed either.

As with any new technology it is important to test all of the functionalities of the system in different and well-defined cases. Therefore it is good to test the system on its own as much as possible before making any new modifications to the UGV platform which can cost a lot of time and money.

The first objective of this thesis is to work out a proper method to determine the contaminations on the sensor's protective cover which will evoke the cleaning process. Second objective is to design several different technical solutions and figure out the pros and cons of each system. Third objective is to test the solutions separately and in combinations to figure out the solutions giving the best result and to test the method for validation described below.

2 Proposed methods

The need for reliable and accurate vision data for autonomous mode is very vital. The problem of detecting and cleaning the lenses of sensors is a new problem for Milrem Robotics which is not taken into account yet. This part of the thesis describes the proposed methods to detect the contamination and to validate the cleaning systems developed.

Obviously there are a lot of factors that can affect the results as well. Accurate dosing of the contamination and vibration from the machine are just a few examples which are not considered during this work due to lack of time. To ensure the validation of the tests proper setup was established during image capturing [17, 18]. This also helps to recreate the scene for future testing by minimizing the factors which can affect the results.

2.1 Contamination detection method

The first method proposed is aimed at detecting the contamination which triggers the cleaning system. This is extremely vital in autonomous mode where the UGV needs to decide on its own when cleaning is needed.

The contaminations under investigation are rain and mud. Other types of subjects like organic matters, oil, bugs and fog are out of the scope of this thesis and need to be discussed in future development.

2.1.1 The rain detector

One of the most common types of extrinsic matter that can contaminate the module are liquids. The likeliest source which needs to be considered is rain. Water can also be splashed on the outer surface of the modules from the tracks. When the temperature falls below zero the water on the surface can form ice.

The proposed technique to detect these types of matters uses the principle of total internal reflection (TIR). TIR happens when a light source with a 45-60 degree angle is beamed on any transparent surface and almost all of the light bounces back to the detector on the same side [19]**.** When a water droplet falls on the outer surface of the glass, some of that light refracts and less light will arrive on to the detector, as seen in figure 2.1 [20, 21, 22].

This kind of system can be created by using a dedicated light emitting diode (LED) light source and a light sensitive photodetector. It is a common system in modern cars [19].

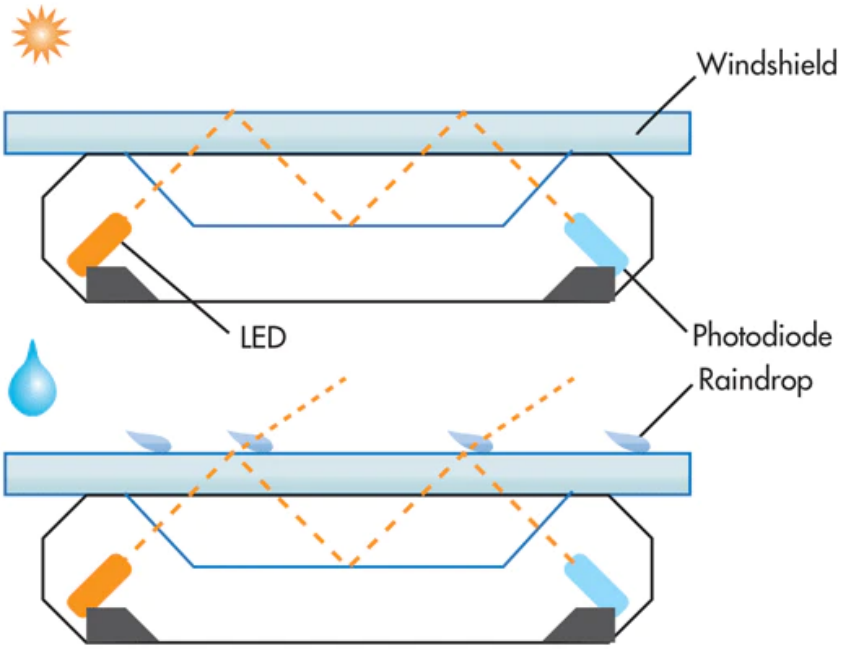

Figure 2.1: Total internal reflection used in most car rain sensors [modified] [22].

The proposed system uses a 940nm infrared (IR) LED and a IR photodiode with daylight blocking filter [23]. In order to maximize the efficiency of this system a circuitry must be created to increase the power of IR LED emission and the sensitivity of the photodiode. Render of the rain detector module can be seen in figure 2.2.

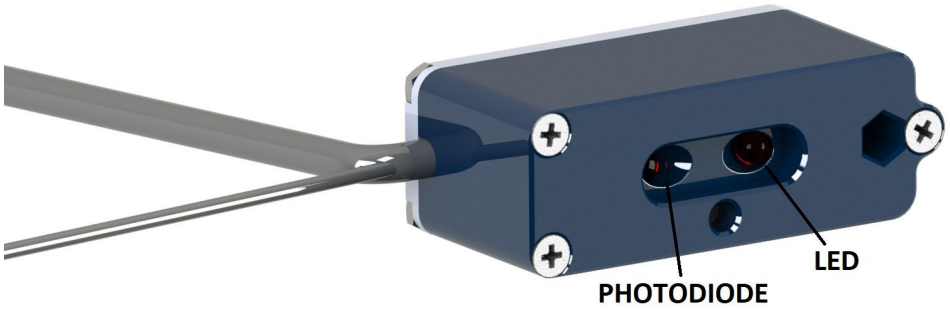

Figure 2.2: Rain detector module render

The light emission system uses the concept of high current pulse generation to increase the emission power. Usually an IR LED can withstand up to 10 times more current than normal when used with pulsed signals with approximately a 1% duty cycle [24]. This maximum

current value can be found in the LED datasheet under Peak Forward Current (I_{FP}) or as the Forward Surge Current (I_{FSM}) [22, 24].

The LED used in this application is LL-503IRC2E-2AC from the company Lucky Light. It has a I_{FP} of 1A with 10% duty cycle and 100 μs Pulse width [22, 24]. This is 900 mA more than can be used in continuous forward current mode.

From the period and duty cycle the maximum pulse duration was calculated:

$$Tmin = Pulse\,Width/Duty\,Cycle = 100\,\mu s/10\,\% = 1\,ms \quad (1)$$

From (1) the maximum frequency is:

$$Fmax = 1/Tmin = 1\,kHz \quad (2)$$

In order to generate 1 kHz signal a NE555 timer was used to create the circuit shown in figure 2.3.

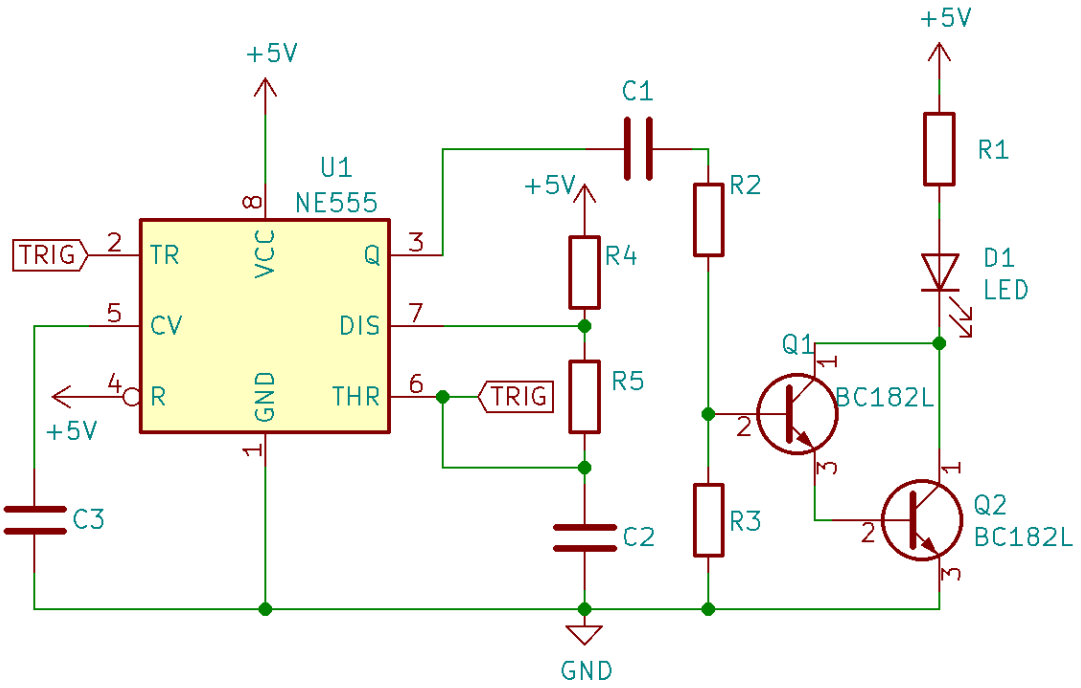

Figure 2.3: 1 kHz pulse generator with IR LED (D1)

The following table shows the component values in figure 2.3.

Component ID	Value or type
D1	LL-503IRC2E-2AC
Q1	BC182L
Q2	BC182L
U1	NE555
R1	5Ω
R2	1kΩ
R3	1kΩ
R4	8.2kΩ
R5	68kΩ
C1	10nF
C2	10nF
C3	10nF

Table 2.1: 1 kHz pulse generator with IR LED components

The generated pulses are then received by the photodiode. Even though the photodiode also works when connected straight to the ADC of the microcontroller, it does not have enough sensitivity in this configuration. The circuit needs a transimpedance amplifier which makes the photodiode sensitive even to the smallest change in light intensity [25]. When the light hits the photodiode a small current is generated which is then amplified and converted into an output voltage which can be read by a microcontroller. The circuit uses an LM358 operational amplifier [26] with negative resistance feedback [25]. Diodes D3-D5 are optional and are used to eliminate saturation of the operational amplifier in presence of a strong external light source.

The gain resistor (R6) is calculated according to formula 3:

$$R6 = \frac{VoutMax - VoutMin}{Ira} = \frac{5V-0V}{60\mu A} = 83k\Omega \quad (3)$$

The bypass capacitor (C4) is calculated according to formula 4:

$$C4 \leq \frac{1}{2 * \pi * R6 * fp} \leq 1.91nF \quad (4)$$

where fp is input frequency.

The figure 2.4 shows the schematic of a transimpedance amplifier used.

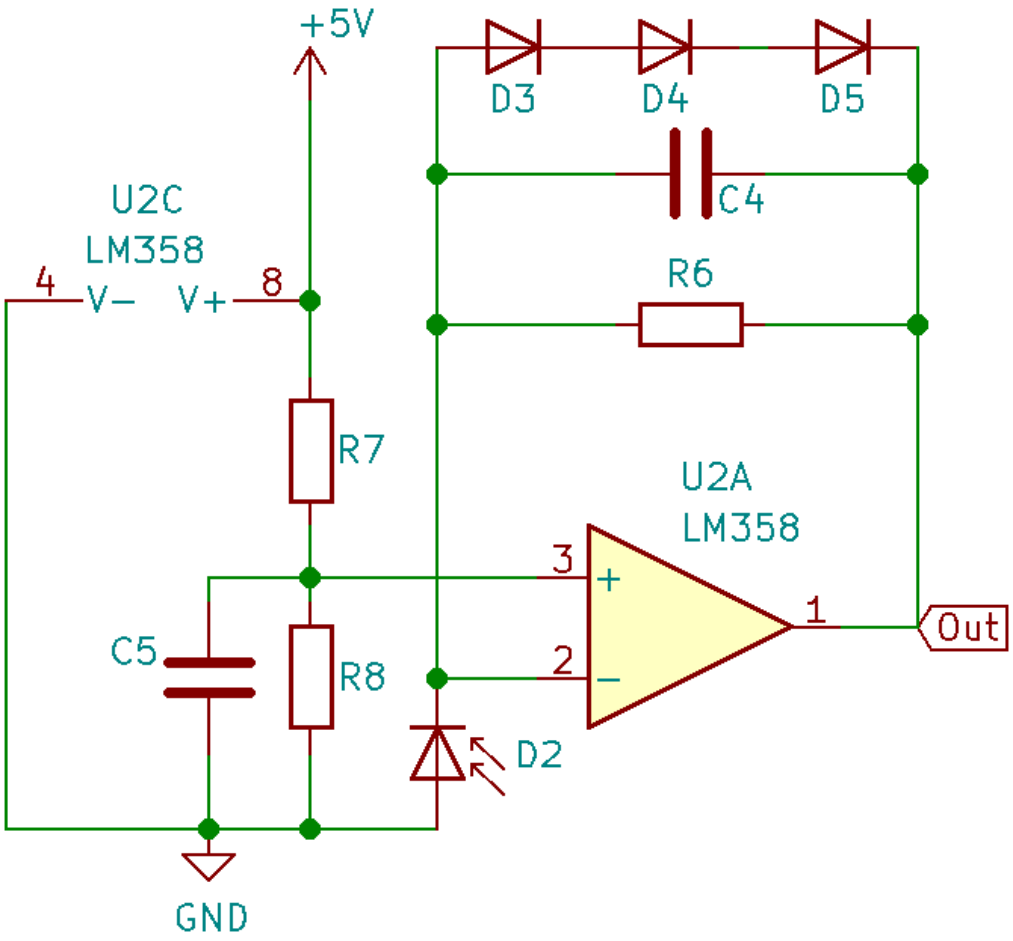

Figure 2.4: Transimpedance amplifier circuit

The following table shows the component values in figure 2.4.

Component ID	Value or type
D2	BPV10NF
D3	US1J
D4	US1J
D5	US1J
U2	LM358
R6	83kΩ
R7	330kΩ
R8	22kΩ
C4	1.8nF
C5	100nF

Table 2.2: Transimpedance amplifier components

When tuning the system the initial value with a window with known cleanliness should be tuned in the middle giving the system ability to detect increase and decrease of signal. The expected values for rain should be considered lower than the middle value.

The detector can be built around a microcontroller like for example Atmega328. This microcontroller is really common in Arduino type prototyping platforms [27]. The custom-made PCB featuring the detectors electronics can be seen in figure 2.5.

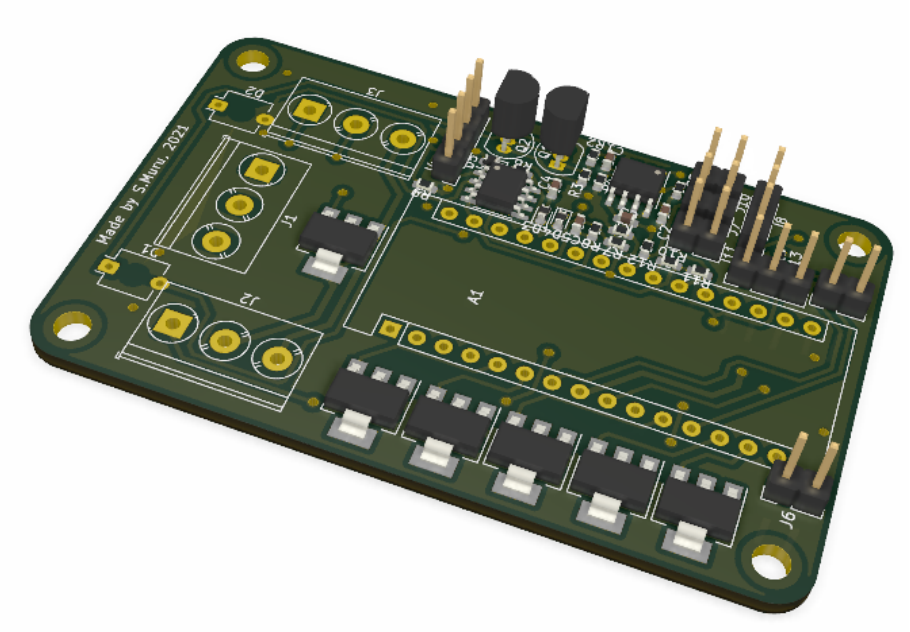

Figure 2.5: 3D render of the custom-made sensor mainboard

2.1.2 Solid particle detector

Like mentioned in paragraph 2.1 the solid particles considered in this thesis is mud. Mud can be considered as grainy dark matter which has the ability to block the incoming light. In this thesis mud is considered as wet dirt.

To detect solid particles four photoresistors placed on the inner surface of the glass were used. With an aperture approximately 12.6 mm^2 the resistors are able to measure the light intensity. The trigger threshold is constantly calculated by taking the mean of all four photoresistors. This helps to eliminate false positives results while driving in different lighting conditions. The chosen cleaning system triggers when the intensity of an individual photoresistors drops below the trigger threshold indicating a blockage in front of its aperture.

The photoresistor works by applying 5V over the pins and uses a light sensitive wire which changes its resistance in presence of photons. This changes the output voltage which is able to be detected by an analog-digital-converter (ADC). [28]

The mud detector stand-alone module and assembly can be seen in figures 2.6 and 2.7.

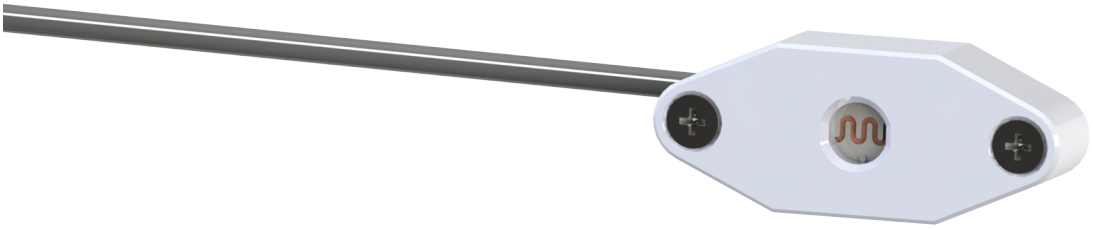

Figure 2.6: Single photoresistor module

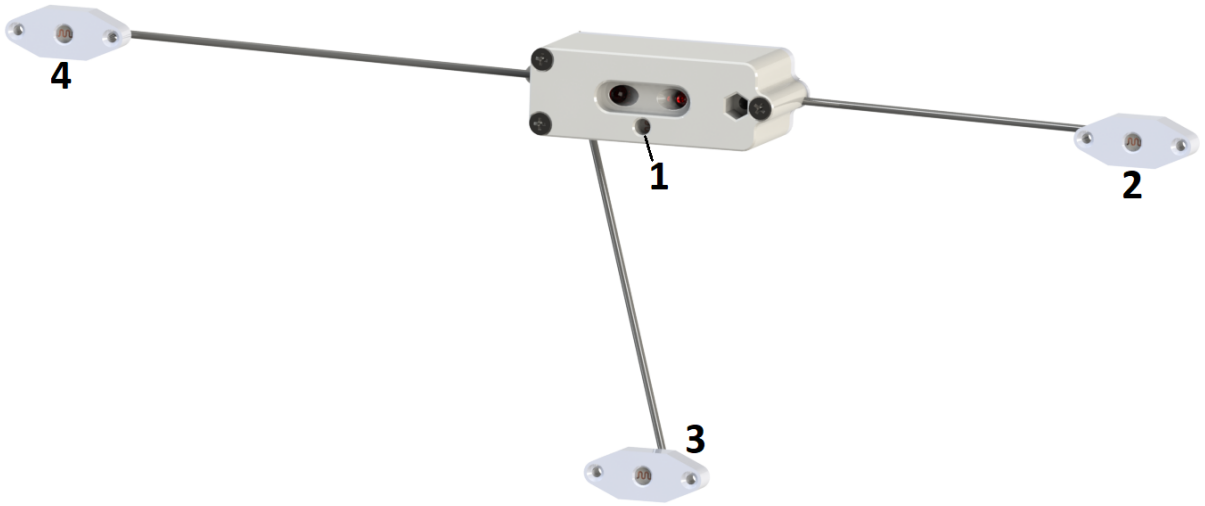

Figure 2.7: Solid particle detector assembly with four photoresistors

2.2 Cleaning efficiency method

The proposed method takes the use of the sensor itself under consideration. Validating the efficiency of the cleaning process is done by taking pictures of dedicated test charts before and after the cleaning process and analysing the image quality from these images. This approach eliminates the need for a separate sensor package to analyse the cleaning efficiency, making the system much simpler.

The downside of this approach is a need for a controlled environment and setup to conduct the measurements to minimize unknown factors as much as possible. Despite that there is no limitation of using the same method actively on the field while driving.

2.2.1 Test setup requirements

Before every image quality test begins it is important to have the camera settings in known configuration and they should stay the same during all of the tests. There are three ways to have them:

1. In default factory settings, which is easy to reproduce
2. Optimized settings from previous experience
3. In configuration from previous experience with an agreeable clean lens

Second key factor is the configuration of the test setup. The room where the tests are done needs to be well ventilated, temperature and humidity should always be measured and documented before and after the test [18, 29]. In order to have an acceptable alignment a proper stand is needed. All the measurements need to be conducted with similar focus distance.

Third key requirement for proper repeatability is consistent lighting conditions. The charts must be lighted from two different sides as shown in figure 2.8.

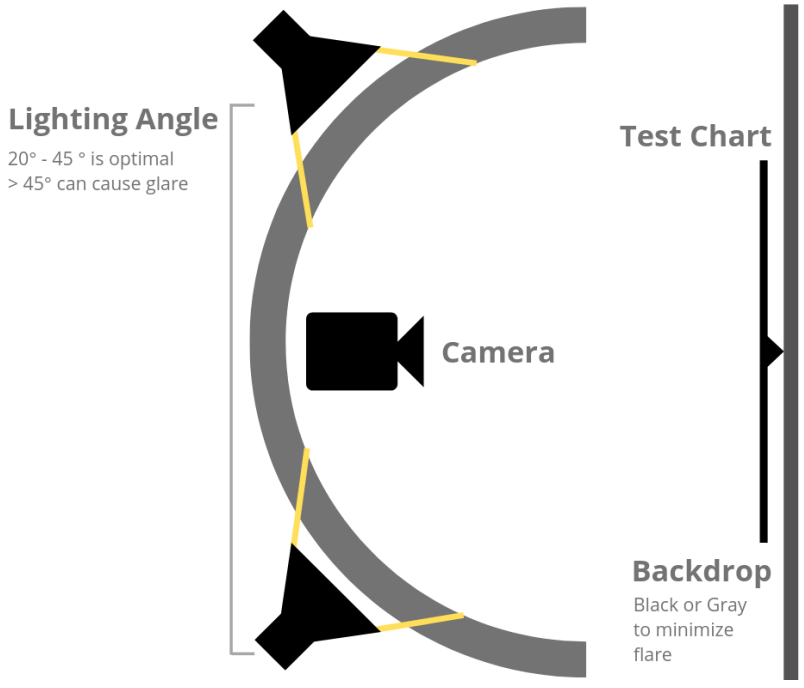

Figure 2.8: DUT, charts and lighting position [18].

Due to the nature of the fisheye lens of the camera the test charts should be placed as shown in figure 2.9. The dark background must cover the whole area behind the test charts and the FOV of the camera to avoid reflection.

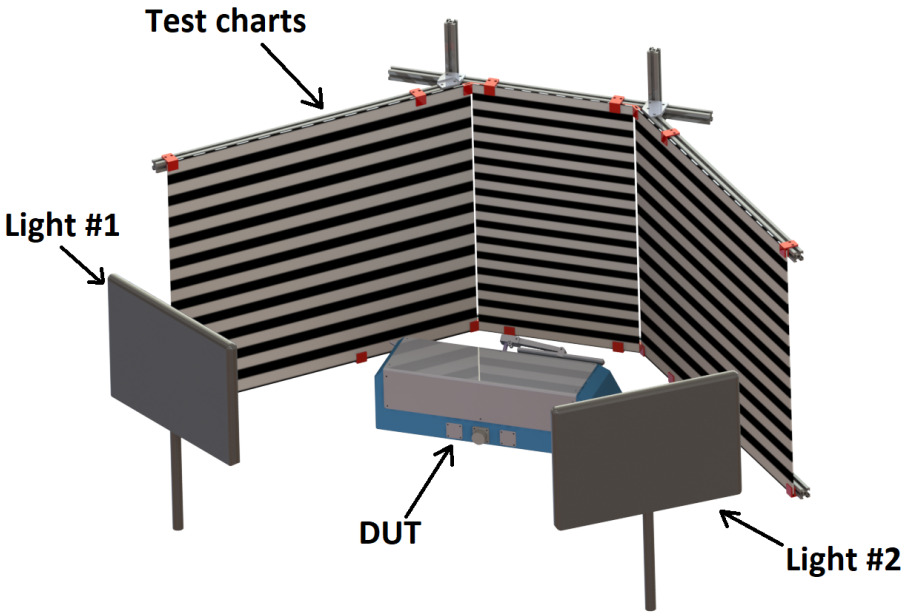

Figure 2.9: Render of the test setup

In order to have consistent results following parameters under control during the tests should be:

1. Constantly or previously ventilated room (to reduce moisture)
2. Temperature: 20 degrees (+-2 degrees)
3. Humidity: 40% (+-3 %)
4. Illumination:
    a. correct position between the DUT and chart
    b. known light bulb type
    c. uniform illuminance
    d. known light temperature
5. Absence of ambient light
6. Reflect-free walls:
    a. dark colour
    b. matt
    c. no reflective surfaces

2.2.2 Blur detection

It is common that computer vision algorithms are built using high quality image datasets [30]. For UGVs on the field this is impossible to achieve while a significant amount of blur is already coming from movement and sharp turns. The added distortion from contamination can worsen the image quality to the point where even deep neural networks (DNN) are not able to determine the scene with needed accuracy. It is shown that existing DNNs are still sensitive to blur (and noise) distortions [30]. The following chapter describes a simple and straightforward way of determining the amount of blur in a digital image.

The analysis procedure takes use of images of striped test charts before and after the cleaning process.

There are several techniques available to detect the blurriness of an image [31, 32, 33]. According to [34] and [35] the variation of the Laplacian was considered the most promising. This simple technique allows us to compute a fine measurable single floating-point result allowing us to compare measurements taken after the cleaning process with the initial results.

Because the convolution can only be done with a single channel image the input image needs to be converted into grayscale. As regular visible light cameras output three channel images (RGB) the process needs to turn the RGB values to grayscale images usually between 0-255 [35].

The next step is to take the second derivative of the image. For this we use the Laplacian operator (6) as the kernel**.** The Laplacian highlights the regions of an image which contains rapid intensity changes [36]. With these changes we are able to determine how much the scene has lost its sharpness.

$$\Delta f = \frac{\partial^2 f}{\partial^2 x} + \frac{\partial^2 f}{\partial^2 y} \tag{6}$$

In the nature of an image which is a 2-dimensional array the Laplacian kernel is the sum of the partial derivatives in x and y direction as shown in formulas (7) and (8).

$$\frac{\partial^2 f}{\partial^2 x} = f(x + 1, y) + f(x - 1, y) - 2f(x, y) \quad (7)$$

$$\frac{\partial^2 f}{\partial^2 y} = f(x, y + 1) + f(x, y - 1) - 2f(x, y) \quad (8)$$

Combination of these equations gives us the 3x3 filter as shown in figure 2.10 [34].

$$\begin{bmatrix} 0 & 1 & 0 \\ 1 & -4 & 1 \\ 0 & 1 & 0 \end{bmatrix}$$

Figure 2.10: The Laplacian operator.

The final step is to calculate the variance of the Laplacian. The result means the value of standard deviation squared. The goal is to calculate the variance of a series of pictures in a row and compare the values before and after the cleaning process.

The process consists of steps in the following order:

1. Import the image with OpenCV
2. Convert the image into grayscale.
3. Calculate the second derivative of the image using the Laplacian kernel
4. Take the variance of this value
5. Compare the values before and after the cleaning procedure.

3 Contamination control solutions

During this thesis several technical solutions were created to remove the contaminants analysed in section 2.1. The main criteria of the solution is its ability to remove the contamination from the outer surface as efficiently as possible according to the method described above.

The second criteria is the overall reliability of the system. The cleaning system cannot limit the usability of the UGV in conditions where THeMIS is currently able to operate and therefore becoming the weakest link in the system. The overall design should consider the robustness of the UGV without any limitations. The modules should be weatherproof and should withstand vibrations and shocks generated by payload or by the machine while driving.

Limitations also came from the design and measurements of the existing robot. The designed module, as seen in figures 3.1 and 3.2, needs to fit under the spoiler of the UGV and all external parts need to be covered when not in use.

Another key consideration is its maintenance capability and ease of access. Every mechanical part encounters some kind of wear during its use and needs some kind of maintenance from time to time to function properly or to stay in its working condition. Maintenance should be able to be done on the field with little to no tools by the operator with according training.

Prior to every operation proper manual cleaning and check-ups should be performed. With a cleaning system using liquids, the liquid container should have easy access for refilling. If different washing liquids are used for different missions the specifying type of fluid should be able to be selected in software to determine the understanding of the systems cleaning capability.

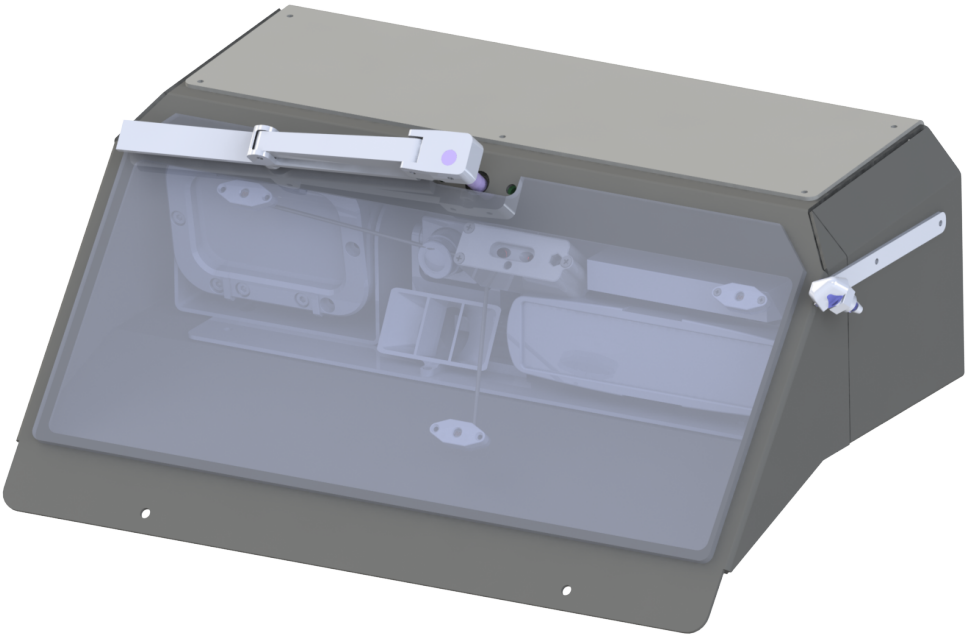

Figure 3.1: Render of the front module

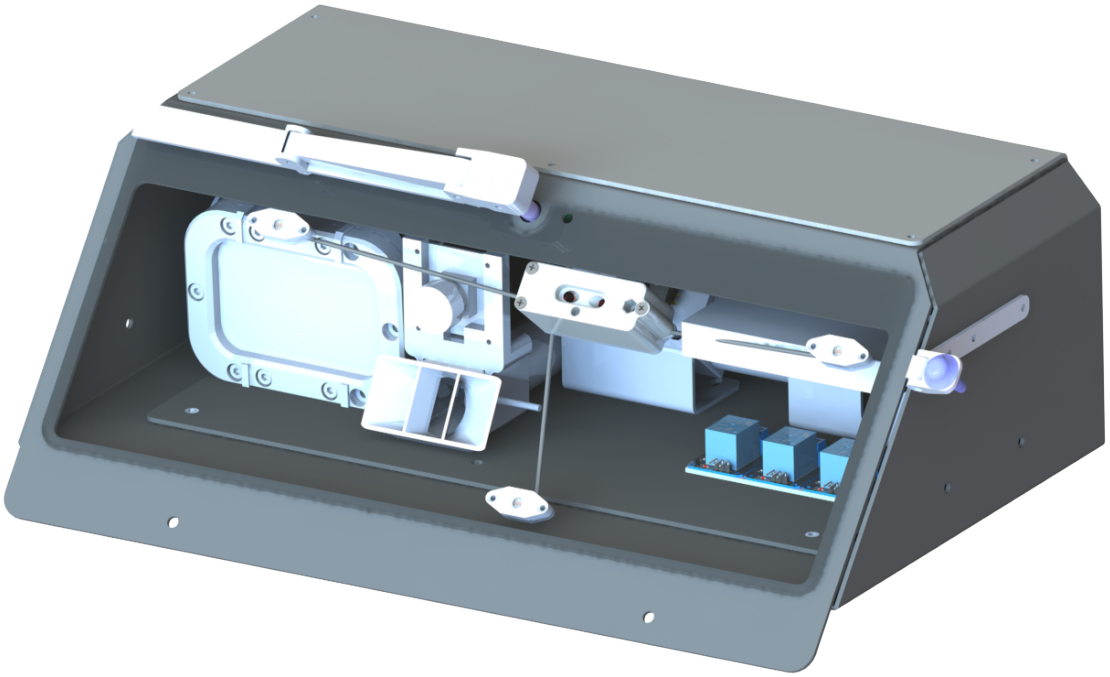

Figure 3.2: Render of the rear module

3.1 Outer surface solutions

The renders of the front module in figures 3.3 and 3.4 show the parts of the outer surface: main frame, shaft seal, shaft seal adapter, front window, bayonet connector and back lid. The metal enclosures are laser cut out of 2mm thick S235 steel sheet. The bended edges are welded together to make a sealed system. The enclosure back lid is attached with M3 countersink screws and sealed with silicone or with other similar waterproof hermetic paste. No custom-made O-rings or seals are needed.

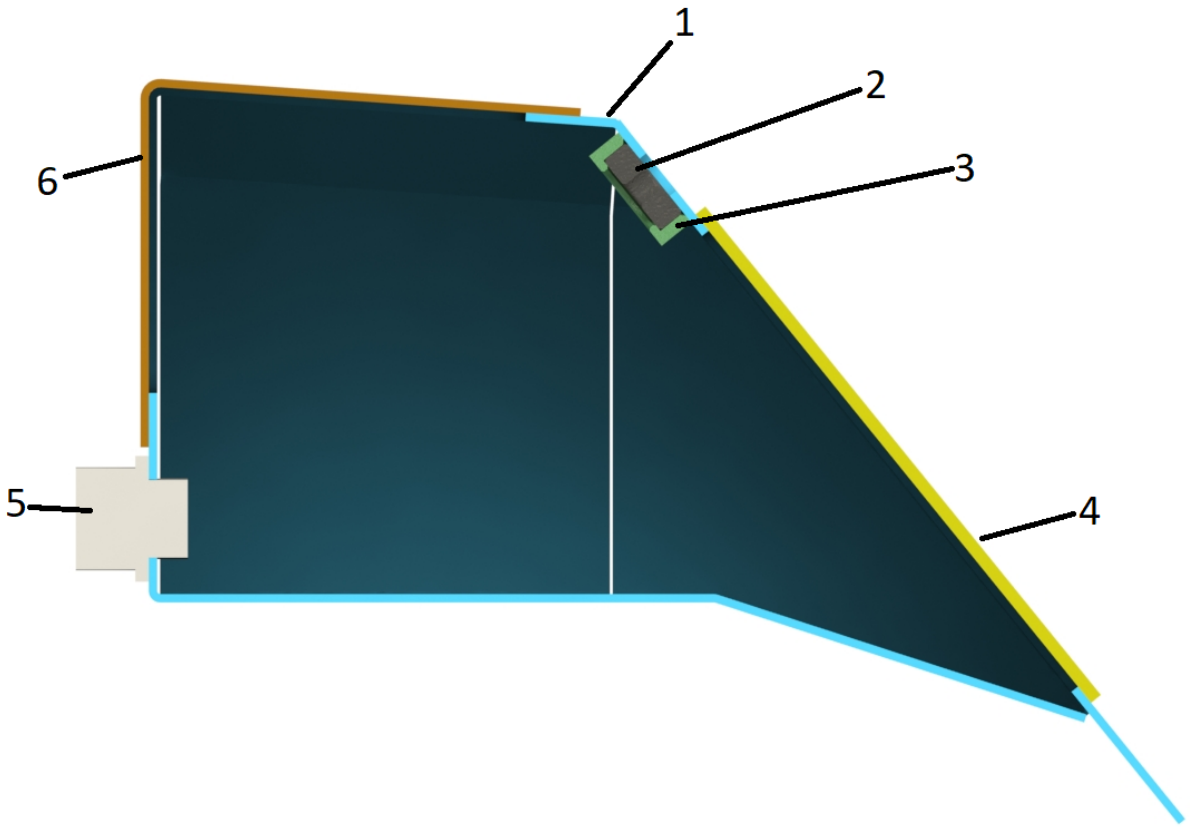

Figure 3.3: The front module enclosure components: main frame (1), shaft seal (2), shaft seal adapter (3), front window (4), bayonet connector (5), back lid (6)

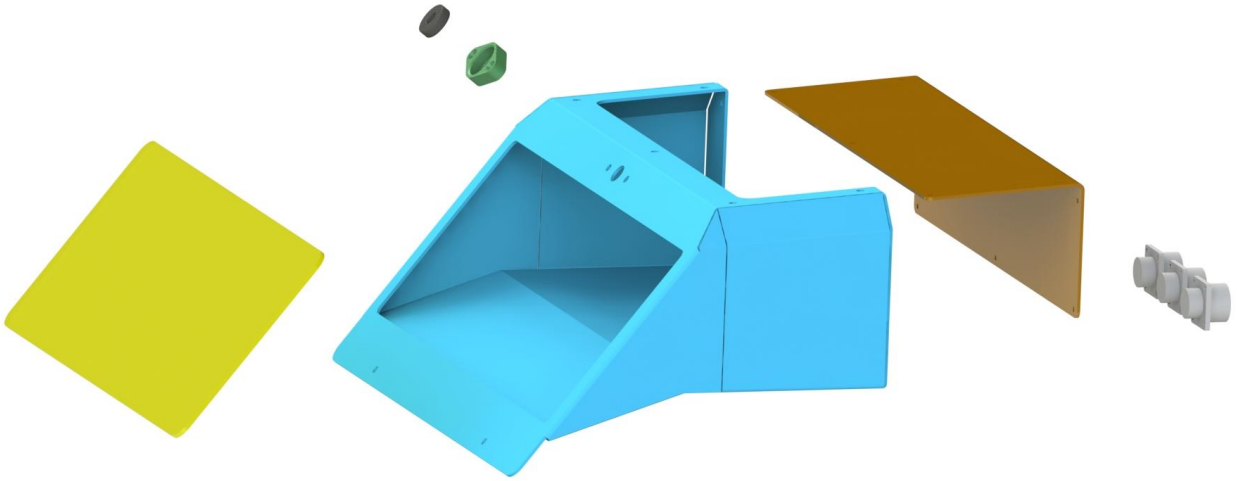

Figure 3.4: The front module enclosure components exploded view

The front window is made out of polystyrene. The window is 4 mm thick. It is glued to the frame using a silicone-based glue. Other impact proof transparent materials can be used as well. The physical and optical properties of polystyrene can be seen in table 3.1.

Parameter	**Value**
Density ρ	1.05
Thermal expansion coefficient α	6.4-6.7
Maximum service temp T_s	80
Thermal conductivity K	2.4-3.3
Water absorption A_{H2O}	0.03
Refractive index	1.5739 @940nm
Abbe number	30.9

Table 3.1: Parameters of Polystyrene [37].

3.1.1 Wiper technology

Wipers are the most commonly used technology in the automotive industry. The wiper can be made out of soft rubber or silicone-like materials to push the dirt and water away from the sensor's field-of-view. The wiper should have a changeable “tool” because they tend to wear out or get damaged. Wiper should be stored in a safe way so it cannot be ripped off when not in use. The tool design should withstand the double motion of the wiper. Motor and shaft must also be weatherproof or sealed in a hermetic enclosure. The wiper can be a stand-alone system or it can also be with an integrated nozzle for compressed air or washer liquids [38][39].

However, this is a rather complex system using a lot of moving parts which tend to easily break under stress. Without a water or compressed air system a wiper can easily scratch the outer surface and leave marks which can degrade the optical parameters of the window.

During this thesis several different wiper solutions were designed. The first solution designed was a simple frame with a rubber flap. This design failed to keep the rubber flap firmly in contact with the glass causing uneven results. To keep the rubber flap in firm contact with the window surface a spring loaded wiper was developed. As an alternative to rubber a fabric cloth solution was designed, but this showed no benefits compared with the rubber. After some testing a spring-loaded wiper with a profiled rubber was chosen for the final analysis. The chosen solution is universal and can be used for both of the modules, as shown in figure 3.5.

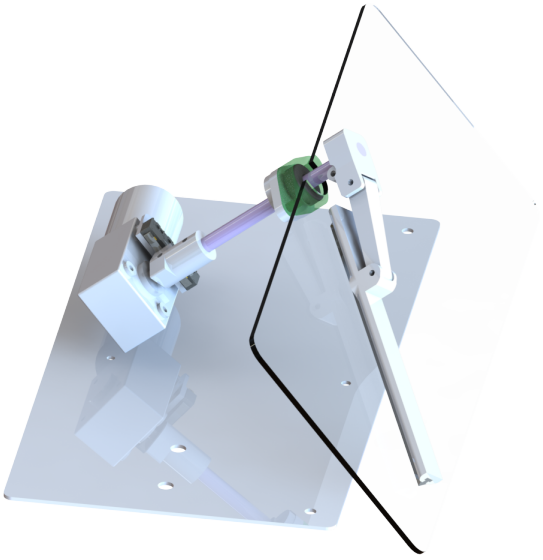

Figure 3.5: Wiper module

Due to limitations of size and shape of the module a single wiper configuration with maximum reach was chosen. Different configurations which were also considered can be seen in figure 3.6. The chosen solution is indicated with red.

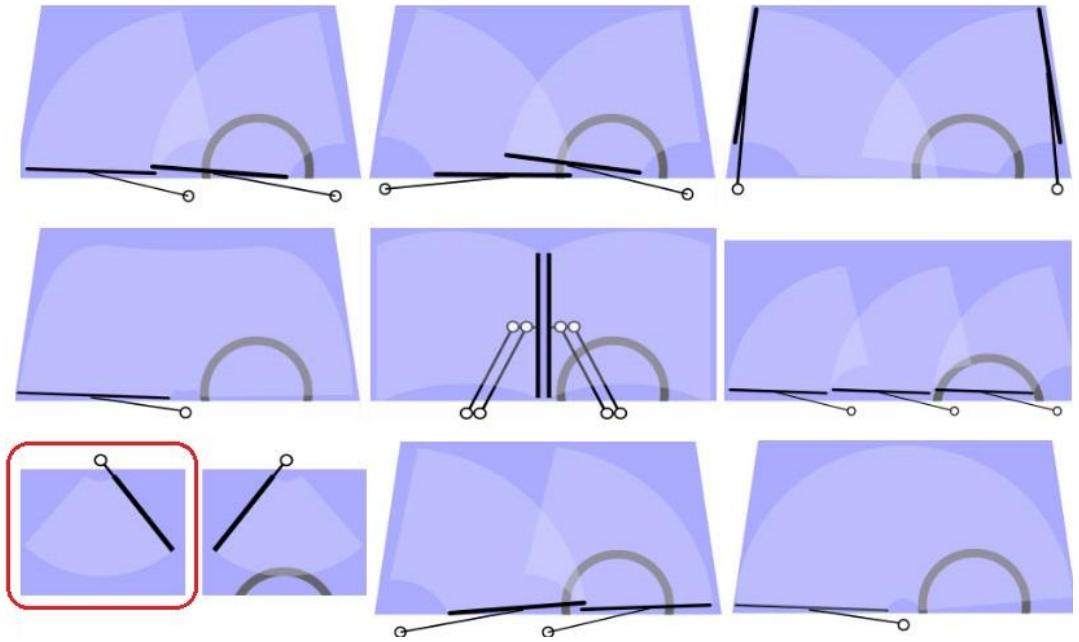

Figure 3.6: Different wiper configurations [modified] [40].

3.1.2 Washing fluid system

Washing fluid or water spray solutions are used in places where wiper technology is not possible or where an extra layer of cleaning is needed. This is another very typical choice in the automotive industry especially with cameras and other sensors. This solution is widely used in the self-driving car industry due to the existence of a washer fluid system built-in in most cars. Windscreens usually use water along with wipers to remove the contamination with more ease.

The advantage of this system is that it has few moving parts. Liquid based washing solutions usually consist of a liquid container, pump, hoses and nozzles, as seen in figure 3.7. Beside a nozzle-based sprinkler, water can also be sprayed to the surface through a perforated tubular system which distributes the liquid more evenly therefore reducing consumption. The nozzles' low-profile design helps it to be easily integrated flush to the mounting surface which makes them less prone to breaking off.

A key consideration for this solution is its limitation of water container size. All of this makes it extra complicated for the UGV with limited space. There will also be a need for constant refill which can be complicated during longer operations.

During this thesis a solution with commercial-off-the-shelf (COTS) nozzles which is typically used in the automotive industry was created. The nozzle was placed outside, on the upper right corner of the module. This simplified the design by not having a watertight interface with the inner side of the module.

The system was built so that different water mixes can be used as the detergent.

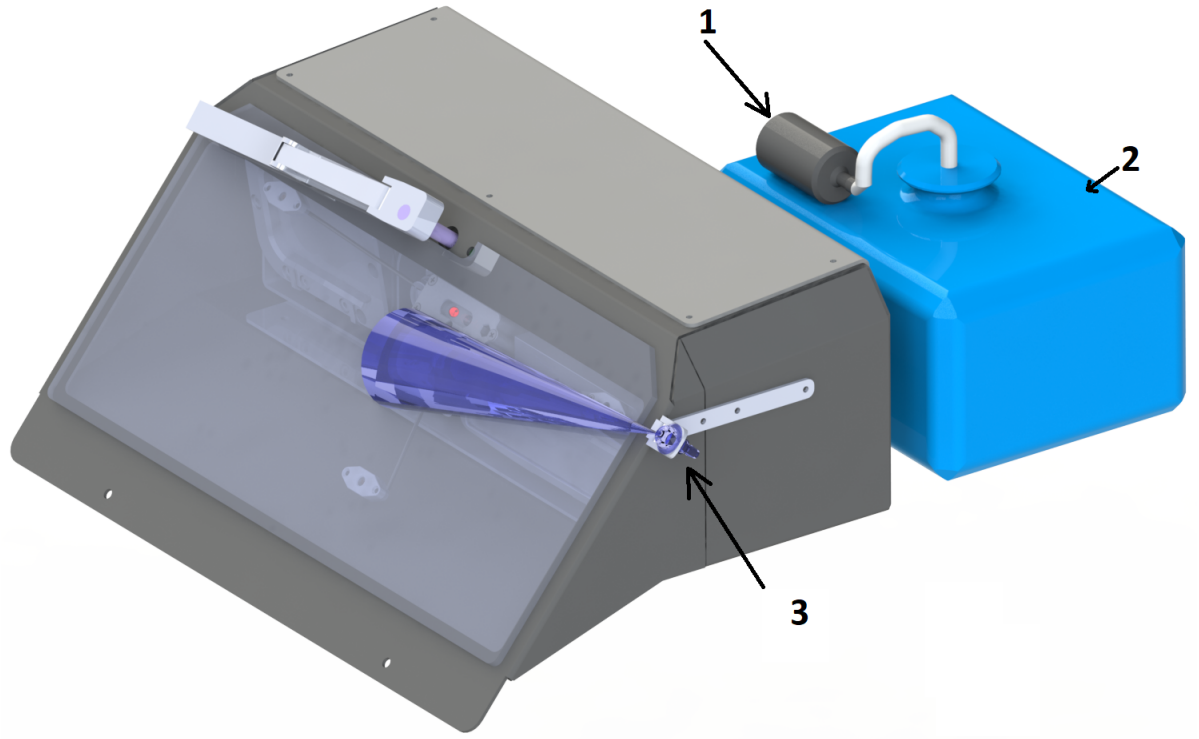

Figure 3.7: The washing fluid solution with water pump (1), water tank (2) and water nozzle (3)

3.1.3 Compressed air system

Compressed air makes use of high-speed air blowing on the surface. This is not so widely used in autonomous vehicle applications but is still a simple and robust solution. Compressed air is used to push the debris away from the sensor area. It can be used parallel with similar nozzles used in liquid-based solutions. Compressed air works great for dirt but can also be good for liquids.

Downside of this system is its noisiness. When air in the compressor gets too low the air pump usually makes a significant amount of noise. This can be a problem in military operations where concealment from the enemy is required.

The system consists of a 12V compressor with 250 PSI pressure. As seen in figure 3.8 the system uses the same nozzle as the water system. When used together a non-return valve can be placed at the intersection of these two systems.

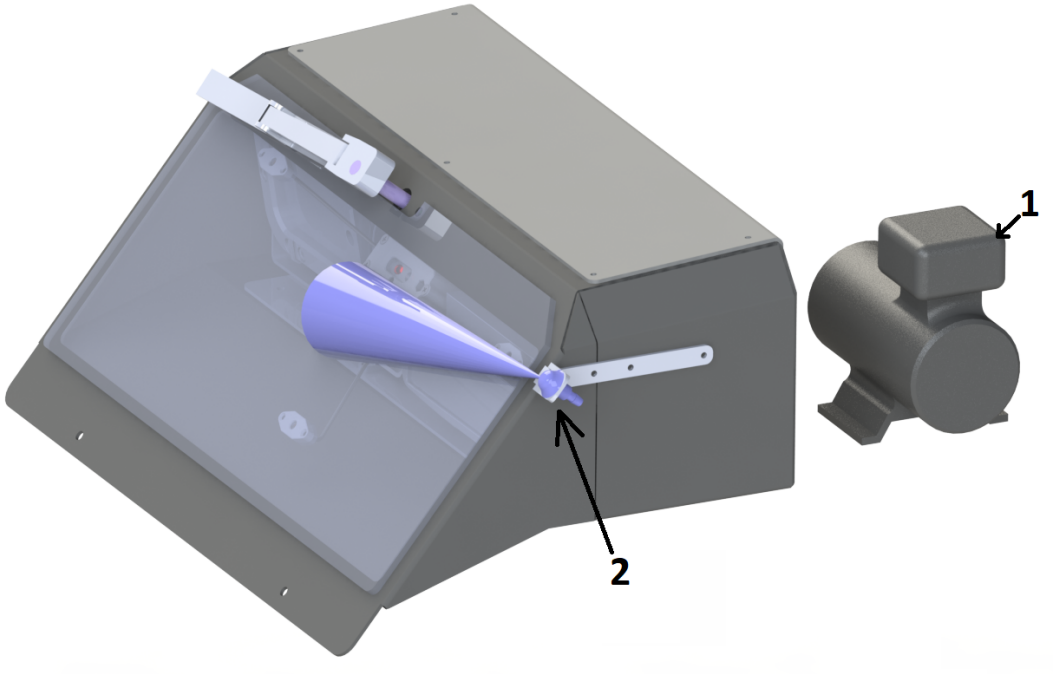

Figure 3.8: Compressed air solutions with air pump (1) and air nozzle (2)

3.2 Inside surface systems

Due to the hermetically sealed compartment the module can witness icing and moisture building up on the inner surface of the glass. In order to prevent the module becoming the limiter of the system, glass heater and moisture detector solutions were created.

3.2.1 Glass heater

Glass heater is a very common solution in de-icing and anti-fog systems. It works against ice and fog which can build up on both sides of the window. In this thesis two technologies to heat the glass were considered:

- integrated tungsten or copper wire on the inner surface of the glass, figure 3.9
- hot air blowers usually in the lower part of the glass, figure 3.10.

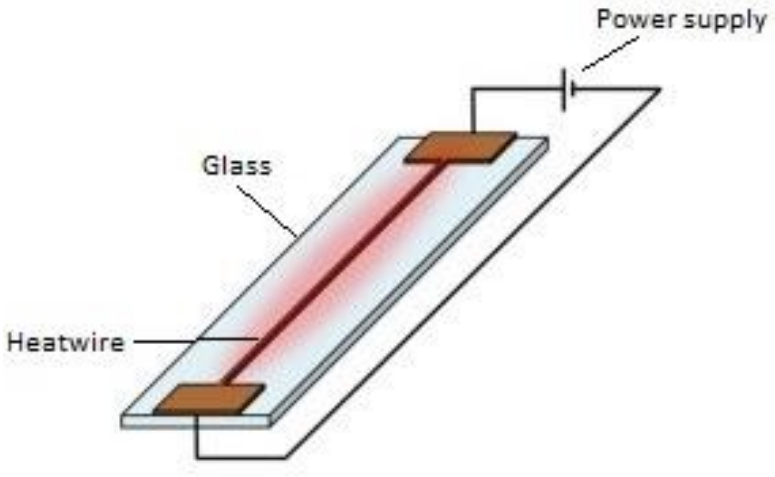

Figure 3.9: Heater module with heatwire [modified] [41].

Due to higher complexity and higher need for customizability the integrated wire solution was not considered. Instead a hot air blower solution using a car 12V cigarette lighter was designed. Its standardized shape and robust design were the main reasons for choosing it as a heating element.

Along with the heat element is a Sonoff SF-DS18B20 temperature sensor which can measure temperature from -55℃ to +125℃ [42]. This is used to turn on or off the heating element to have a constant temperature of air flow which also can be adjusted in the software.

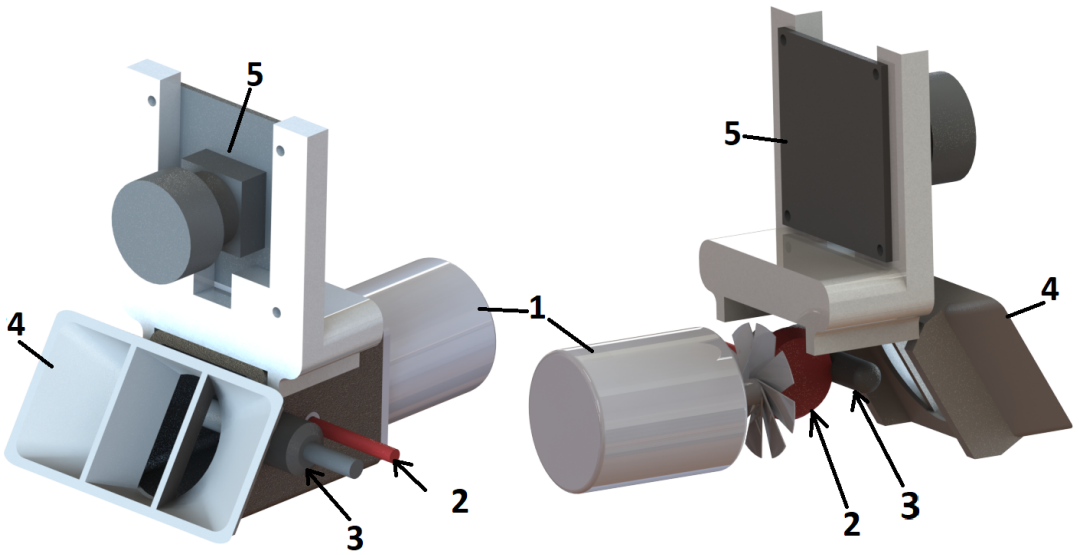

Figure 3.10: Heater module with camera mount - fan motor (1), heat element (2), temperature sensor (3), air funnel (4) and camera (5)

3.2.2 Moisture detection

Because there is a sealed compartment, moisture can build inside the module when the temperature inside drops lower than ambient air temperature. Measurements of this temperature difference are needed to control condensation and protect the electronics from moisture which can cause short circuits. Moisture on the sensor lens and modules window can also cause negative effects on image quality.

The system consists of a humidity sensor DHT22, as seen in figure 3.11. This can be used to indicate to the operator when there has been a problem with the window or seals of the module.

Along with the heater module described above the moisture can be controlled by the temperature inside the module. With the use of the ventilator and a one-way air breather valve the moist air can be transported out from the module.

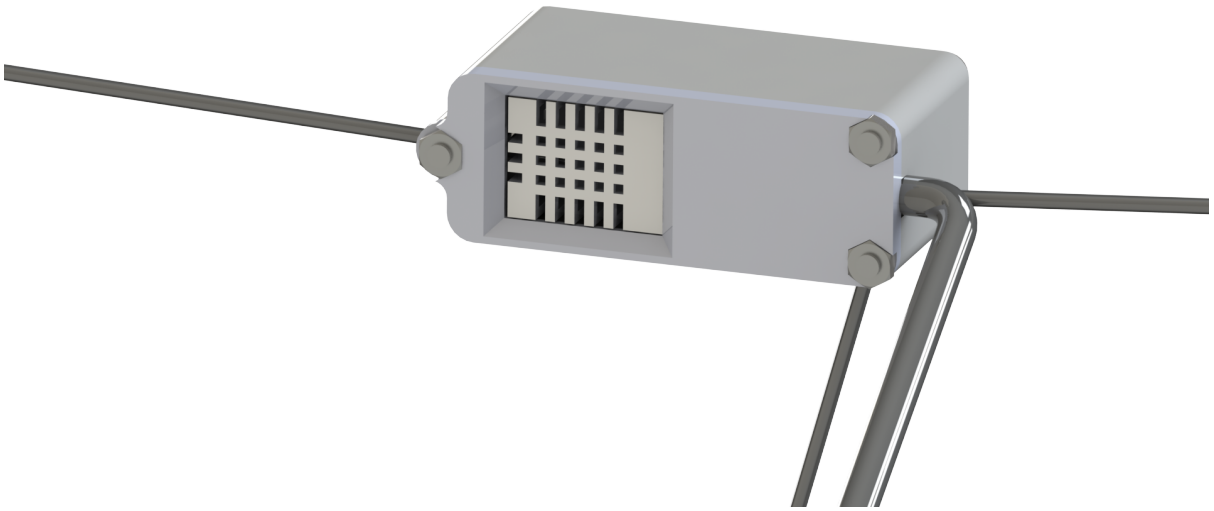

Figure 3.11: The DHT22 humidity sensor

4 Testing

Testing was performed in and around Tartu Observatory in April and May 2021. The testing contained blur detection analysis for both of the modules in a dedicated environment following the requirements mentioned in paragraph 2.2.1. Due to their similar design the sensor packages were installed and tested only with the rear module.

The final results and conclusions are divided into two categories. The first being the detector's reliability to initiate the cleaning system without operator input in different lighting conditions. Second category consists of analysis to determine the efficiency of the cleaning systems on the outer surface of the module and its effect on image quality using the proposed method described in paragraph 2.2.

The finished modules can be seen in figures 4.1 and 4.2.

Figure 4.1 Finished front module

Figure 4.2 Finished rear module

4.1 Detectors

The contamination detector packages were tested by calculating the number of successful detections from the total attempts. In order to test the sensor's efficiency a total of 30 tests were done in two different lighting conditions (low level and high level). The light levels were determined by the photoresistor's average value. The light level condition was set to 30% from the sensor's maximum and minimum value.

The threshold levels for both systems were tuned during daylight and were unchanged throughout the testing period.

4.1.1 Rain detector

The liquid contamination was applied to the outer surface by a spray bottle. This formed a series of small droplets of water, imitating rainfall as seen in figure 4.3. The nozzle location and angle were kept unmoved throughout the test. The liquid used in testing was regular tap water.
Success criteria for each attempt was an output signal which fell below the set threshold and initiation of the cleaning system was activated.

The reaction time of the detection was limited to 10 seconds, meaning that if the system was not able to detect the liquid contamination within this time the attempt was considered a failure.

Figure 4.3 Rain detector testing in a high light environment

Out of the 30 attempts in the final test the success rate of the rain detector was:

- Low lighting condition - 27/30
- High lighting condition - 26/30.

The rain detector showed equally good results in both light environments. The failed attempts were probably caused by the water droplets sliding off in front of the sensor before the triggering function got called before the time limit was reached.

4.1.2 Mud detector

As mentioned in paragraph 2.1.2 four photoresistors were placed around the FOV of the camera in order to measure the light intensity of the surrounding environment. The cleaning system is triggered when one of the sensor's values falls under a certain threshold.

As seen in figure 4.4 the mud used in this test was made using a mixture of planting soil and water. The dosing of the mud was approximately 50 ml and was applied equally to the surface by a drop from above. This ensured the likeliest scenario where the mud is thrown at the module by the track.

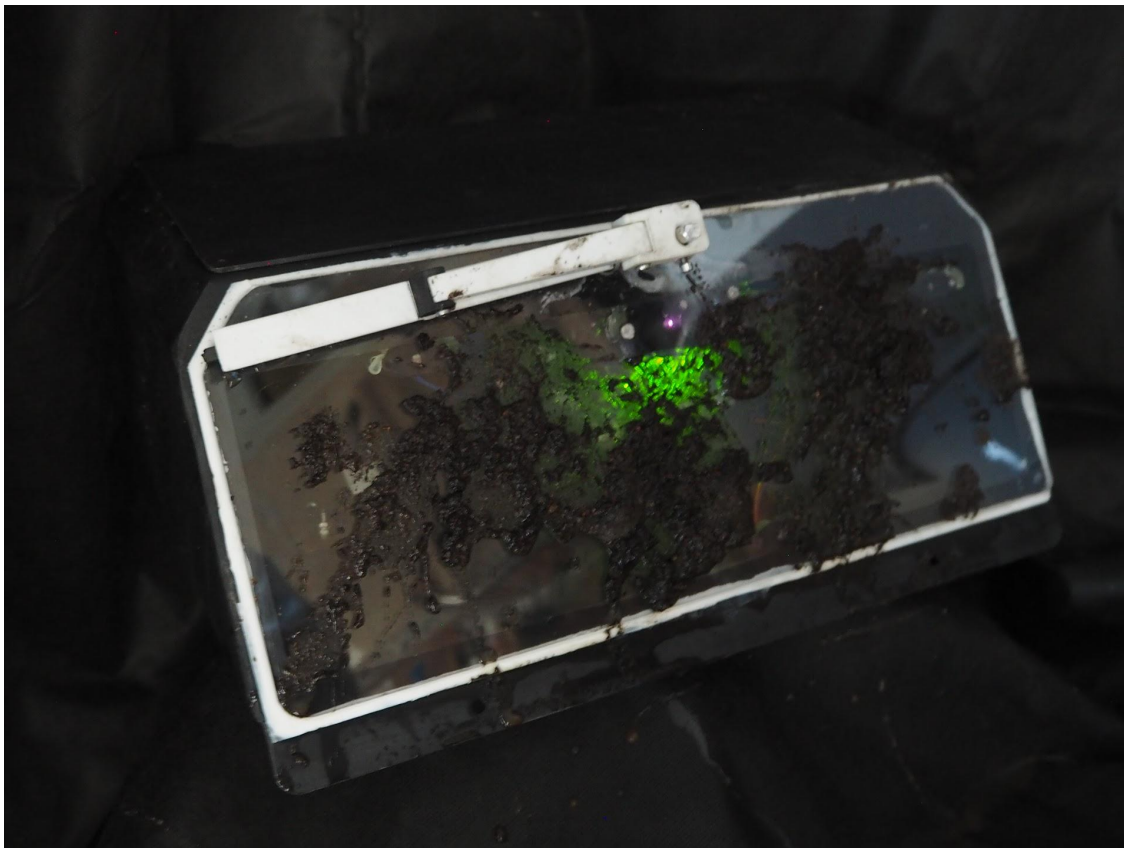

Figure 4.4 Mud detector testing in a low light environment

From the 30 attempts the final score for the mud detector were:

- Low lighting condition - 27/30
- High lighting condition - 29/30.

The mud detector success rate slightly dropped in lower light conditions due to triggering value not falling below threshold level when the blockage by the contamination was not complete. A minimum operating level was set at the point where the presence of ambient light dropped too low, showing no effect on the trigger output.

4.2 Sensor analysis

The sensor under investigation is the UGVs main cameras facing to the rear and front of the tracked module. Due to technical difficulties and image conversion limitations a different camera with similar parameters was used in the test.

The camera used is called ELP-SUSB1080P01-L36 and can be seen in figure 4.5. It has a 120-degree fisheye lens, similar to that used by Milrem Robotics. The camera had no ability to change its parameters and was considered being in default configuration. The camera was able to produce pictures with 1080p resolution. The image output extension was .jpg. [43]

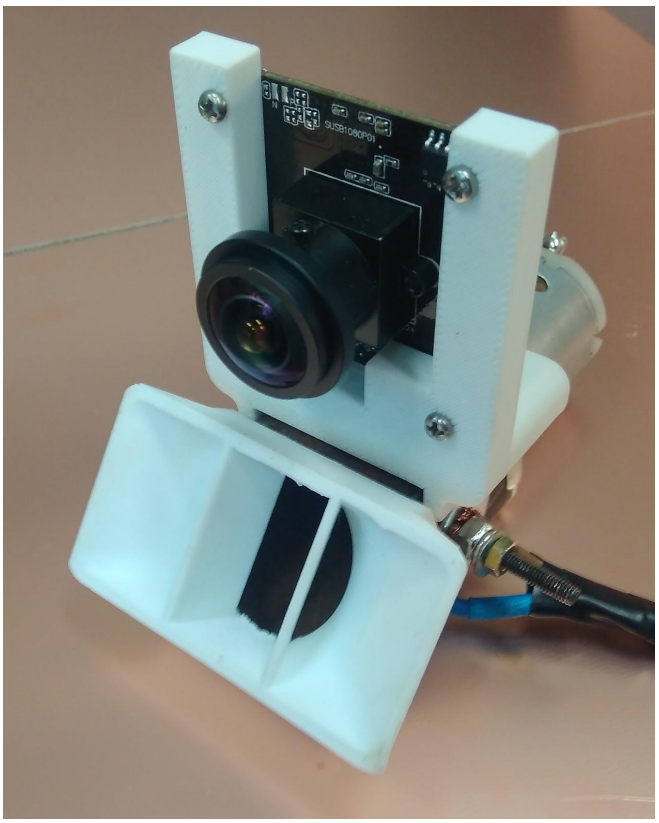

Figure 4.5 Picture of the camera module

4.2.1 Test setup

The tests were conducted in a 6 square meter room with no windows. The room had good overhead ventilation. The temperature and humidity stayed within 20 °C (±2 °C) and 40% (±2 %), respectively throughout the test. The walls were covered with dark fabric to reduce any reflection from the FOV of the camera. Any openings from ambient light were sealed off.

The backlights used in the setup were a set of Dazzne D50 LED panel lights [44]. They provided 6500 K light which is the black body temperature of the Sun [45]. The light intensity was set to 65% which gave the highest resolution.

The test setup can be seen in figure 4.6.

Figure 4.6 The test environment

4.2.2 Software and test charts

The software used to calculate the variance of the Laplacian was written in Python. It uses the help of the open-source image processing library called OpenCV. [35]

The stand was built using a 20x20 mm aluminium frame with a set of custom-made brackets holding the test chart. The focus distance for the camera aperture to the centre of the test charts was 200 mm. As seen in figure 4.7 the test chart used in this thesis consists of black and white horizontal stripes with 2 mm line thickness.

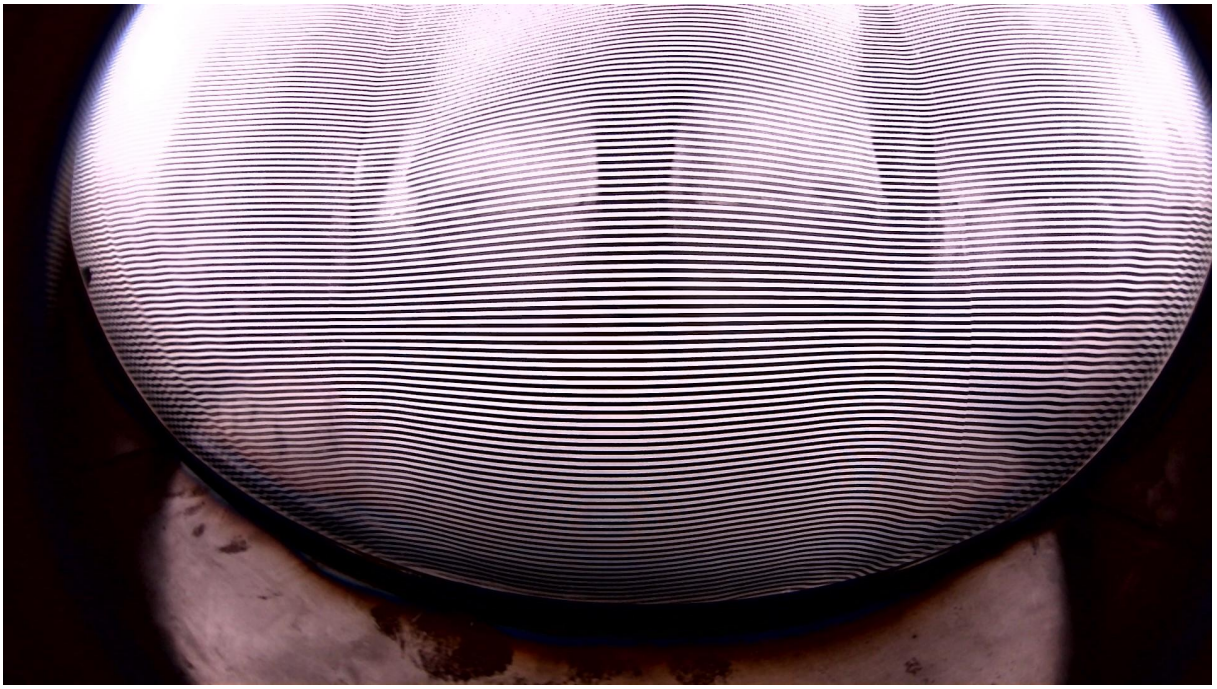

Figure 4.7 Picture of the test chart before the test

4.2.3 Measurement results

The following paragraph shows the measurements of the camera after cleaning water and mud. Total of 25 images were taken before and after the cleaning and calculated their average value. The results were plotted against each other as shown in figures 4.8 to 4.10. Total of 10 attempts were conducted. The yellow line indicates the initial value of the results while the camera was placed outside the module. The black line shows the measure after applying the contamination. The red line indicates the number at the beginning of the attempt and the green line indicates the final result.

When applying the contaminants similar technique was used as described in paragraphs 4.1.1 and 4.1.2.

The test sequence for the rear module was:

1. Wiper vs Rain
2. Wiper vs Mud
3. Wiper and water sprinkler vs Mud.

After witnessing severe degradation of the window outer surface, the test sequence for the front module was changed to 1, 3 and 2. This helped to determine the degradation level while applying the water spray system before using the wiper.

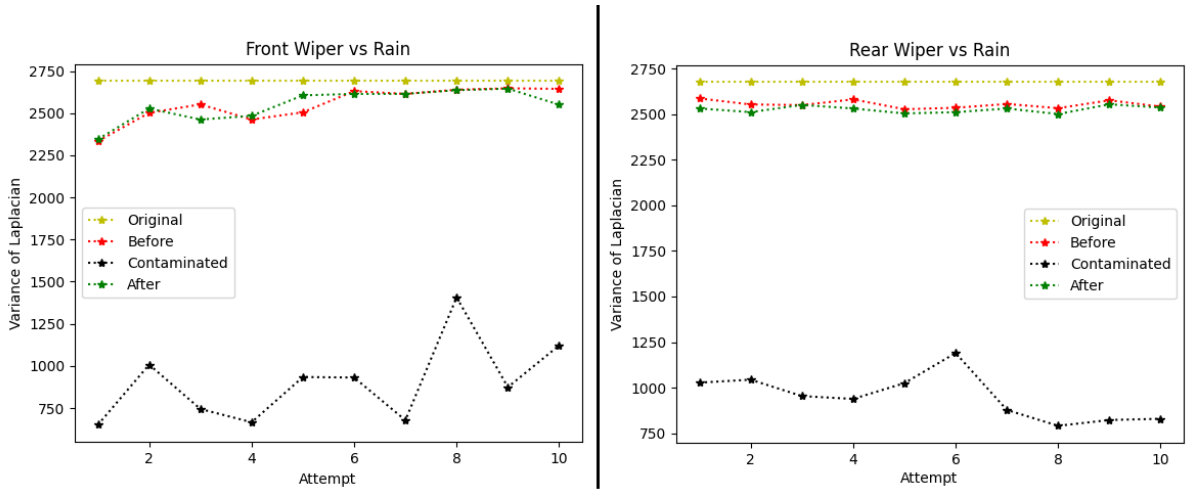

Figure 4.8 Wiper against rain

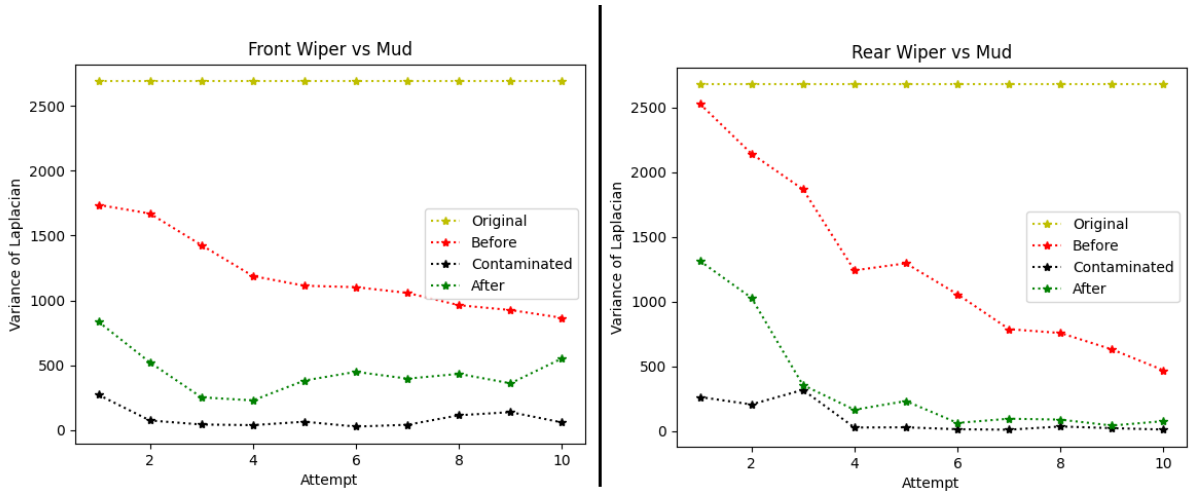

Figure 4.9 Wiper against mud

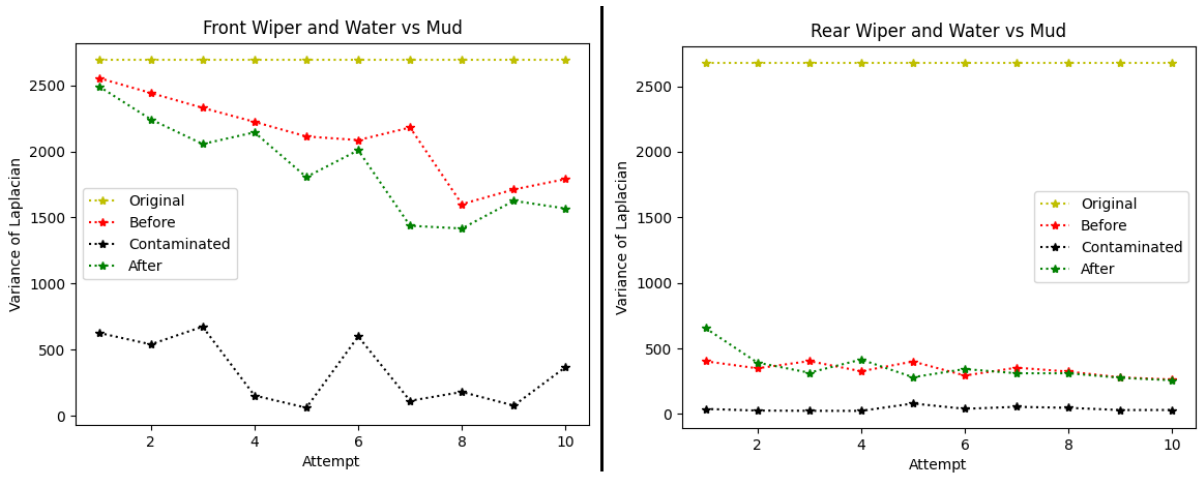

Figure 4.10 Wiper and water sprinkler against mud

4.3 Analysis and future work

During the image analysis a total of 4710 data points were collected. The overall design and cleaning systems configuration achieve the set goals. For both of the modules the wiper system showed excellent results against water contamination. Using the wiper and water sprayer together showed good results cleaning the mud contamination.

As shown in figures 4.9 and 4.10 there was a significant increase of blur throughout the test while trying to clean the mud. This was caused by the mud particles scratching the outer surface of the window. This means that the polystyrene window used is not suitable for this application and needs to be replaced with other more durable material.

The testing of the compressed air system showed no positive effect against both of the contaminants. The final conclusion was that this system needs a different nozzle or higher air pressure.

The water system against mud showed significant ineffectiveness as a standalone system. It was able to wash away small particles of mud but was struggling with bigger particles. The solution might work with water jets with higher power. The wiper technology as a standalone system showed relatively poor results against mud.

The detectors modules showed good results detecting the contaminants. Total of three threshold levels were determined. For further fine tuning more data in different lighting conditions is needed.

The glass heater and moisture detector modules were able to keep the fog and moisture level at desired set value. The system's reliability with different temperature and humidity values should be tested in a larger variety of environments.

The module needs to be tested with the lights inside to see the reflection effect on the camera. The future work should also consist of testing the modules reliability against vibrations produced by the UGV while driving. The modules should also be tested with a larger variety of contaminants as mentioned in paragraph 2.1.

Conclusion

The aim of this thesis was to develop a set of technical solutions which are able to protect and clean the field-of-view of any data acquiring system used by the Milrem Robotics UGV. The contaminants under investigation were water and mud.

For this two enclosed modules were designed which accommodate the sensors and navigation light which are located at the front and rear of UGV. In order to determine the contamination on the window of the module methods for the sensor package were proposed. For determining the cleaning systems efficiency a suitable method was presented.

Second part of the work focused on the development of the sensor package and different cleaning system technologies. A set of systems for the inner surface of the module's window were also designed.

In the third part the sensor package and cleaning systems for the outer surface of the window were tested by the method mentioned above.

From these analyses the results showed the systems strong sides and pointed out the problems. The overall design of the modules proved to be working. The cleaning systems against water contamination showed good results. For contamination of physical particles the system showed limitations in cleaning and degradation of the window surface. The suggestions for improvements were made and documented.

Acknowledgements

I would like to thank my supervisor Hendrik for making sure this thesis is at the level needed.

I would like to especially thank my fiancée Piia for all the support and love.

A great appreciation goes also to the people at Tartu Observatory and Milrem Robotics for their tremendous work and achievements in Estonian space and robotics industry.

Bibliography

[1] "The lifesaving power of semi-autonomousUGV technology", *in Global Military Communications Magazine, (February 2018).* http://www.satelliteevolutiongroup.com/articles/UGV.pdf

[2] T. Litman, "Autonomous Vehicle Implementation Predictions: Implications for Transport Planning", (March 2021).

[3] B. Pal, S. Khaiyum and Y. S. Kumaraswamy, "Recent advances in Software, Sensors and Computation Platforms Used in Autonomous Vehicles, A Survey", *in IJRAR, Volume 6, Issue 1 (March 2019).*

[4] National Research Council, "Technology Development for Army Unmanned Ground Vehicles", pp 98-99, (2002).

[5] A. Bouhraoua, N. Merah, M. AlDajani and M. ElShafei, "Design and implementation of an unmanned ground vehicle for security applications", *in Proceeding of the 7th International Symposium on Mechatronics and its Applications, (April 2010).*

[6] D. M. Tilbury and A. G. Ulsoy, "Reliable Operations of Unmanned Ground Vehicles: Research at the Ground Robotics Reliability Center", (January 2010).

[7] Milrem Robotics, About us, (visited 05.01.2021). https://milremrobotics.com/about-us/

[8] Milrem Robotics, Defence, (visited 05.01.2021). https://milremrobotics.com/defence/

[9] A. Reschka, "Safety Concept for Autonomous Vehicles", *in Autonomous Driving - Technical, Legal and Social Aspects, pp 473-496, (May 2016).*

[10] P. Koopman, "Autonomous Vehicle Safety: An Interdisciplinary Challenge", in IEEE Intelligent Transportation Systems Magazine (Vol. 9, #1, Spring 2017, pp. 90-96).

[11] P. Saithibvongsa and J. E. Yu, "Artificial Intelligence in the Computer-Age Threatens Human Beings and Working Conditions at Workplaces", *in Electronics Science Technology and Application, Volume 5, Issue 3 (2018).*

[12] A. Kravchenko, “AI, Robotic and the Workplace of the Future”, (2019).

[13] Milrem Robotics, Nutikas UGV, (visited 05.01.2021). https://milremrobotics.com/nutikas-ugv/

[14] C. Harper and G. Virk, “Towards the Development of International Safety Standards for Human Robot Interaction”, *in Int J Soc Robot 2: pp. 229–234 (2010).*

[15] R. Wu, S. Yan, Y. Shan, Q. Dang and G. Sun, “Deep Image: Scaling up Image Recognition”, (MAy 2015).

[16] S. Dodge and L. Karam, “A Study and Comparison of Human and DeepLearning Recognition PerformanceUnder Visual Distortions”, (May 2017).

[17] D. Wueller, U. B. Kejser, “Standardization of Image Quality Analysis –ISO 19264”

[18] Imatest, Test Lab setup, (visited 20.02.2021), https://www.imatest.com/solutions/Test-lab-setup/

[19] Encyclopaedia Britannica, “Total internal reflection”, (visited 12.02.2021), https://www.britannica.com/print/article/600414

[20] Carpike Tech, “How Rain-sensing Wipers Work In a car?”, (visited 13.02.2021).” https://carbiketech.com/rain-sensing-wipers/

[21] S2-06 Science Blog, “Application of Total Internal Reflection”, (August 2011), (visited 13.02.2021), http://sst2011-s206sci.blogspot.com/2011/08/application-of-total-internal.html

[22] J. Martinez, “Build Your Own IR Windshield Rain Sensor”, (December 2017), (visited 13.02.2021). https://www.electronicdesign.com/markets/automotive/article/21805970/build-your-own-ir-windshield-rain-sensor

[23] Silicon PIN Photodiode datasheet, (visited 13.02.2021). https://www.vishay.com/docs/81503/bpv10nf.pdf

[24] LL-503IRC2E-2AC datasheet, (visited 13.02.2021). https://www.tme.eu/Document/8d4d369fec521adcb494da36fa782bc9/LL-503IRC2E-2AC.pdf

[25] Texas Instruments, ”Transimpedance amplifier circuit” , (visited 14.02.2021). http://www.schematicsforfree.com/archive/file/Analog/Op-Amps/Transimpedance%20Amplifier.pdf

[26] LM358 datasheet, (visited 14.02.2021). https://www.onsemi.com/pdf/datasheet/lm358-d.pdf

[27] “From Arduino to a Microcontroller on a Breadboard”, (February 2015), (visited 15.02.2021), https://www.arduino.cc/en/Tutorial/BuiltInExamples/ArduinoToBreadboard

[28] LDR07 data sheet, (visited 18.02.2021). https://www.tme.eu/Document/f2e3ad76a925811312d226c31da4cd7e/LDR07.pdf

[29] Imatest, Photography Lab Setup, (visited 20.02.2021). https://www.imatest.com/solutions/photography-lab-setup/

[30] S. Dodge and L Karam, “Understanding How Image Quality Affects Deep Neural Networks”, *in Eighth International Conference on Quality of Multimedia Experience (QoMEX), (April 2016).*

[31] J. L. Pech-Pacheco, G. Cristóbal, J. Chamorro-Martínez and J. Fernández-Valdivia, “Diatom autofocusing in brightfield microscopy: a comparative study”, *in ICPR (2000).*

[32] S. Pertuz, D. Puig and M. A. Garcia, “Analysis of focus measure operators for shape-from-focus”, *in Pattern Recognition, pp. 1415-1432, (November 2012).*

[33] K. De and V. Masilamani, “Image Sharpness Measure for Blurred Images in Frequency Domain”, *in International Conference of DESIGN AND MANUFACTURING (IConDM), pp. 149-158, (2013).*

[34] Sagar, “Laplacian and its use in Blur Detection”, (visited 01.03.2021). https://medium.com/swlh/laplacian-and-its-use-in-blur-detection-fbac689f0f88

[35] A. Rosebrock, “Blur detection with OpenCV”, (visited 20.04.2021). https://www.pyimagesearch.com/2015/09/07/blur-detection-with-opencv/

[36] R. Bansall, G. Ra and T. Choudhury, “Blur Image Detection using Laplacian Operator and Open-CV” *in Proceedings of the SMART (2016).*

[37] Parameters of Polystyrene, (visited 20.02.2021).
https://polymerdatabase.com/polymers/polystyrene.html

[38] “What is Mercedes-Benz Magic Vision Control®?”, (visited 20.02.2021).
https://www.arrowheadmb.com/blog/what-is-mercedes-benz-magic-vision-control/

[39] “Wiper installed spray nozzles”, (visited 20.02.2021).
https://www.speich.com/portfolio_page/wiper-installed-spray-nozzles-nautical/?lang=en

[40] Wiper solutions image, (visited 21.02.2021).
https://99percentinvisible.org/app/uploads/2017/04/wiper-solutions.jpg

[41] Heated glass image, (visited 21.02.2021).
https://ars.els-cdn.com/content/image/1-s2.0-S0920586118311830-ga1.jpg

[42] Sonoff DS18B20 datasheet, (visited 24.02.2021).
https://www.sonoff.ee/ee/ds18b20-3/

[43] ELP-SUSB1080P01-L36 datasheet, (visited 24.04.2021).
http://www.elpcctv.com/high-speed-usb30-industrial-digital-camera-full-hd-low-illumination-camera-usb-elpsusb1080p01l36-p-114.html

[44] Dazzne D50 LED Panel Light datasheet, (visited 27.04.2021).
http://www.dazzne.com/product/show/9

[45] Blackbody radiation, (visited 27.04.2021).
http://gsp.humboldt.edu/OLM/Courses/GSP_216_Online/lesson1-2/blackbody.html

Appendices

Appendix A - The rain detector module

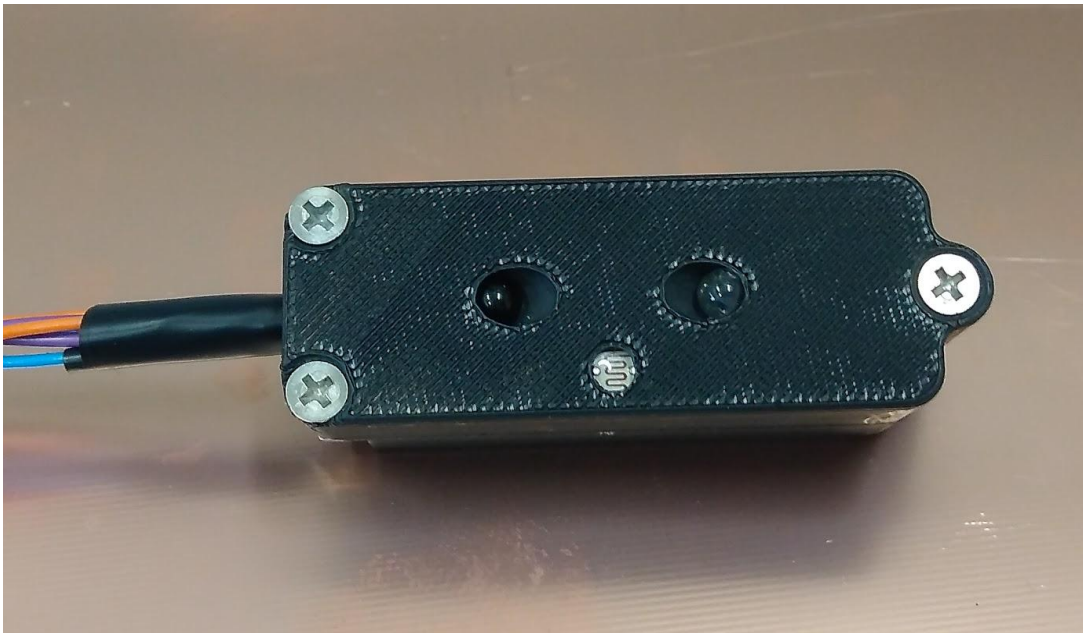

Appendix B - The mud detector module

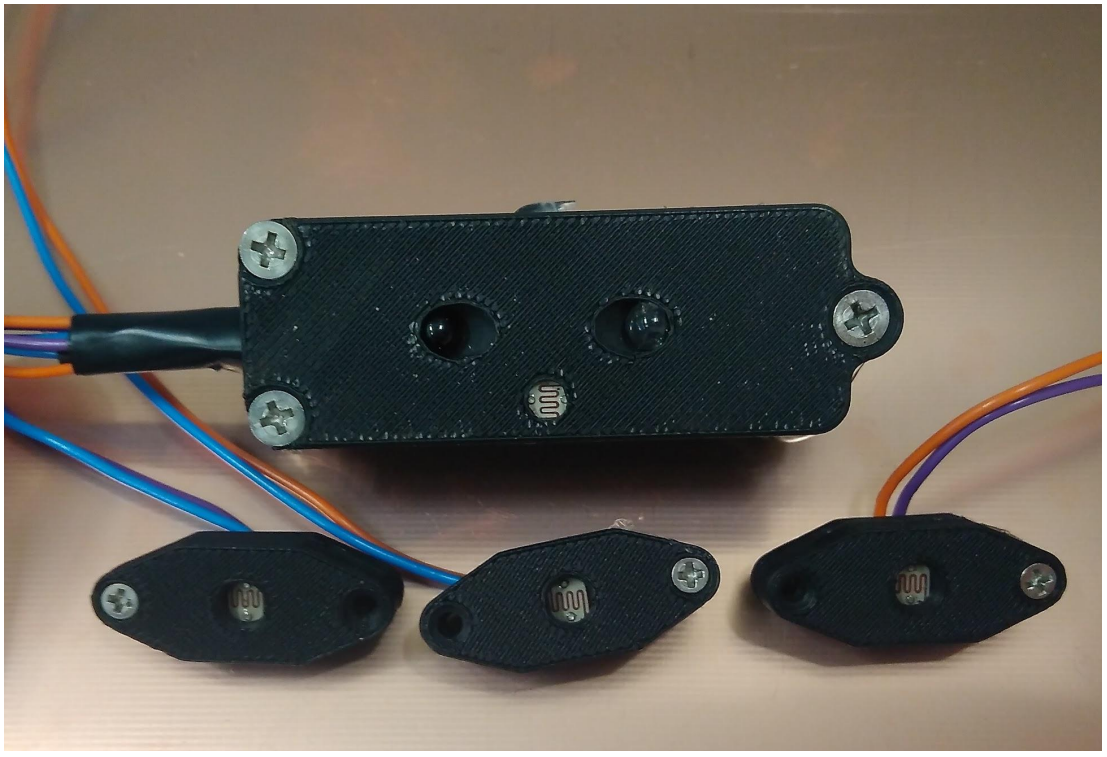

Non-exclusive licence

I, Silvar Muru,

1. herewith grant the University of Tartu a free permit (non-exclusive licence) to reproduce, for the purpose of preservation, including for the purpose of preservation in the DSpace digital archives until the expiry of the term of copyright,

Methods and implementation of contamination control on Milrem Robotics UGV sensors,

supervised by MSc Hendrik Ehrpais.

Publication of the thesis is not allowed.

2. I am aware of the fact that the author retains the right specified in p. 1.

3. This is to certify that granting the non-exclusive licence does not infringe other persons' intellectual property rights or rights arising from the personal data protection legislation.

Silvar Muru,
Tartu, May 20, 2021